Article

In-Plane Shear Behavior of Unreinforced Masonry Wall Strengthened with Bamboo Fiber Textile-Reinforced Geopolymer Mortar

Roneh Glenn D. Libre Jr. [1,*] , Julius L. Leaño Jr. [2], Luis Felipe Lopez [3], Carlo Joseph D. Cacanando [3], Michael Angelo B. Promentilla [4] , Ernesto J. Guades [5], Lessandro Estelito O. Garciano [1] and Jason Maximino C. Ongpeng [1]

1   Department of Civil Engineering, De La Salle University, Manila 0922, Philippines
2   Department of Science and Technology, Philippine Textile Research Institute, Taguig 1631, Philippines
3   BASE-Bahay Innovation Center, Makati 1231, Philippines
4   Department of Chemical Engineering, De La Salle University, Manila 0922, Philippines
5   School of Engineering, University of Guam, Mangilao, GU 96923, USA
*   Correspondence: roneh_librejr@dlsu.edu.ph

Abstract: Old structures that are made of adobe or brick walls are usually unreinforced and not designed for lateral forces. In-plane loads applied to unreinforced masonry walls (URM) are the usual cause of damage and failure of old buildings. In this research, small unreinforced brick masonry wallettes, 350 mm × 350 mm and 50 mm in thickness, are strengthened using bamboo fiber textile and plastered to the face of the walls using short bamboo fiber-reinforced geopolymer mortar. The wallettes are subjected to diagonal shear tests as described by ASTM E519 to investigate the in-plane shear performance of the strengthening method. The performances of 5 wallettes strengthened on one-side with mortar only, 5 wallettes on both-sides with mortar only, 5 wallettes with textile plastered on one-side only, and another 5 wallettes with textile plastered on both-sides, are compared to 5 control specimens without any strengthening. It is observed that the wallettes strengthened on one side and both sides with textile yield an increase in shear of about 24% and 35% in average, respectively. Failure modes show that the usual failure for URM is running bond failure and for strengthened URM is columnar failure. The implications of the results can be used in developing textile-reinforced geopolymer mortar systems to strengthen URM walls.

Keywords: bamboo fiber textile; Carbon footprint; diagonal shear; geopolymer mortar; in-plane shear; strengthening

1. Introduction

The design of old structures such as old masonry churches and heritage structures are usually not made to resist lateral loads, making them vulnerable to seismic actions [1]. For the rising occurrence of earthquake events, protecting heritage structures has been a part of continuous research that aims to substantially reduce the damage that these structures can suffer from seismic activities. Parisi and Augenti [2] made account of the types of damages to cultural heritage buildings caused by earthquake. The majority of the failure modes include the collapse of a portion of the structure, loss of masonry integrity, and in-plane damage to the main façade. A typical failure that was observed for URM walls is in in-plane shear. Retrofitting and strengthening interventions are required to make the masonry wall act as a part of the system to dissipate the lateral forces brought by seismic activities. This will enhance the building resistance and achieve the required seismic safety level in most structural codes [3].

1.1. In-Plane Shear

The collapse mechanism of heritage structures follows out-of-plane and in-plane mechanisms. Failure mechanisms of walls are influenced mainly by the quality and strength of the connection between the walls and the other structural elements. If better connections are implemented, out-of-plane mechanisms are usually prevented, and the critical element becomes the in-plane mechanism [3]. Design provisions for out-of-plane shear response are established, while strengthening for in-plane shear is more complex [4]. In the current study, the strengthening of walls for in-plane diagonal shear is being explored.

1.2. Strengthening Methodologies

There are different methodologies for strengthening reinforced and unreinforced walls. Strengthening URM buildings includes traditional methods such as surface treatments, shotcrete [5], reinforced high performance mortar [6], prestressing with steel bars/ties, and grout injections. An alternative technique is by Steel Fiber-Reinforced Mortar (SFRM) coating that is reinforced with short fibers that are shorter than the coating thickness and randomly distributed in the mortar matrix [1]. Other common methods are the use of externally bonded fiber-reinforced polymers (FRP) and surface coatings reinforced with grid reinforcement. The strengthening includes the used of mesh carbon fabric [7], glass fiber-reinforced plastic (GFRP) [8], and polyparaphenylene benzobisoxazole (PBO) fiber grid [9] covered by epoxy-based adhesive or normal strength mortar. Protecting heritage structures must also include the protection of the environment. This can be achieved through the usage of different innovative approaches of repair and strengthening for old structures. The call for more environmentally friendly construction materials is stimulated by the need for energy-efficient construction with minimal carbon footprint. Nowadays, the use of natural fibers on mortar and concrete is being explored along with the use of geopolymers to lessen the use of conventional cement binder—which contributes largely to the carbon emission. The application of bamboo fibers as reinforcement for developing mill scale (MS)- and fly ash (FA)-based geopolymer composites and as textile reinforcement is being explored as its fibers exhibit attractive mechanical properties and shows competitive results. In the current study, a proposed textile system made of MS and FA geopolymer reinforced with bamboo fiber is used as an innovative repair system for URM walls. The textile system will give the structure strength against lateral loading and improve the walls' performance in the dissipation of lateral loads.

One of the major challenges in implementing interventions for heritage structures is the idea of protecting their cultural and aesthetic value. Studies of Lourenço et al. [10] highlighted the importance of following the recommendations made by organizations that protect the cultural heritage of old architectural buildings. Such structures require in-depth analysis and planning to provide structurally sound engineering techniques that can withstand seismic activities without hampering the historic and aesthetic value of the structure. In the recommendation of the International Council on Monuments and Sites (ICOMOS, 2001) [11], a detailed inspection of the crack pattern may provide the load paths within a structure, thus providing specific areas of target for strengthening intervention. Petrozzi et al. [12] made use of a strengthening technique that is aesthetically acceptable. In their study, the application of strengthening mesh by Blondet et al. [13] is adapted, placing the mesh externally against the walls in the form of straps along the corners of the wall to control the formation of cracks. The recommendations also follow the standard framework for seismic evaluation of existing buildings governed by the Federal Emergency Management Agency (FEMA) and the American Society of Civil Engineers (ASCE). The process includes the selection process of performance objectives to be used, the level of seismicity through spectral response acceleration and Peak Ground Acceleration (PGA), as-built information, structural design, and retrofitting. The strengthening method using externally bonded mesh is adapted for the current study using the proposed bamboo fiber-reinforced textile geopolymer system.

1.3. Determination of In-Plane Shear through Experimental Tests

There are several studies that cited ASTM E519 or the standard test method for diagonal tension (shear) in masonry assemblages for investigating in-plane shear performance of walls [14]. Sagar et al. [15] investigated the shear performance of 350 mm × 350 mm × 78 mm-thick small wallette specimens strengthened with a fabric-reinforced cementitious matrix. It is observed that strengthening one side of the wall yields an eccentric distribution of force and strengthening both sides is ideal. In a study by Oskouei et al. [16], in-plane behavior of various retrofitted URM walls was also investigated. A control specimen that was unreinforced and wallette specimens reinforced with mortar coating, mesh reinforcement, and polypropylene (PP) bands were subjected to shear tests. The dominant failure mode was found to be in the form of diagonal shear cracks, while the wallettes retrofitted with mortar-coated GFRP mesh were found to be performing better than other specimens.

The response of walls is defined with its stress and strain under a certain load [17]. Generally, shear stress can be obtained by the general formula (Equation (1)) below, and deriving the forces as shown in Figure 1 will lead to the specific formula of computing in-plane shear stress (Equation (2)).
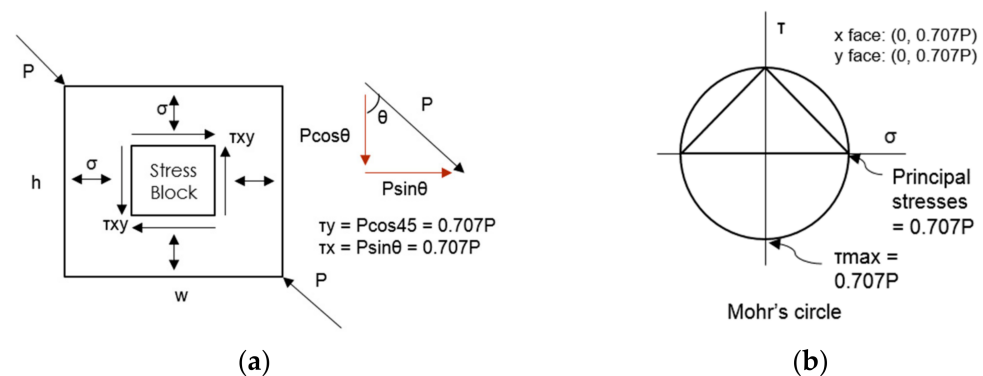
$$Ss = \frac{F}{An} \tag{1}$$

where,

Figure 1. (**a**) Free-body diagram for in-plane shear; (**b**) Mohr's circle based on the forces.

Ss = shear stress, MPa
F = Applied force, KN
An = Net area net cross-horizontal section of the panel.

$$Ss = \frac{0.707P}{\frac{1}{2}t(L+H)} \tag{2}$$

where,

t = thickness of wall
L and H = dimensions of the wall
P = diagonal force measured experimentally
while the shear strain can be obtained by

$$\gamma = \frac{\Delta V + \Delta H}{g} \tag{3}$$

where,

ΔV = diagonal shortening along the axis of applied force
ΔH = diagonal elongation measured perpendicular to the axis of applied force
g = gauge length.

In the current study, URM wallette specimens reinforced with bamboo fiber textile coated with short bamboo fiber-reinforced geopolymer mortar were subjected to diagonal

shear testing to evaluate the increase in shear capacity after strengthening. The comparisons between strengthening one side only and strengthening both sides, with and without bamboo fiber textile, are presented. The resulting shear modulus of each type is used in existing analytical models to verify the experimental results. The experimental/analytical ratios are also presented.

2. Materials and Methods

In the current study, in-plane shear tests for small wall specimens were conducted. The shear performance of small wall specimens, 350 × 350 mm, made of clay bricks, were investigated through the procedures described by ASTM E519 [14]. The clay bricks manufactured from Rizal, Philippines were tested under compression, as described with the standards for testing brick and structural clay tile or ASTM C67 [18]. The in-fill mortars were tested under compression, as described by the procedures of construction evaluation of mortars for plain and reinforced unit masonry or ASTM C780 [19], with a 1:6 cement–sand ratio and a 0.4 mass water–cement ratio, and the strength is in comparison with type O mortar (2.4 MPa), as described by the standard specification for mortars or ASTM C270 [20].

2.1. Materials

This study used the mill scale (MS) powder and the low calcium Class F fly ash (FA) precursors discussed by Libre et al. [21]. The MS-FA proportions on the geopolymer paste activated using sodium hydroxide (NaOH) flakes with 98% purity obtained from Taiwan and sodium silicate in the form of waterglass (WG) were used to develop fiber-reinforced geopolymer mortar as a mortar coating for unreinforced walls. Bamboo fibers extracted from Kawayan Tinik using 5% NaOH solution and treated with 10% aluminum sulfate solution are used as the short fibers and fiber textile reinforcement.

2.2. Parameters

Following the study of Libre et al. [21], the parameters used include the NaOH-to-WG ratio (1:2.5 by weight), whereas the water–solid ratio was kept constant at 0.3 by weight and the activator-to-precursor ratio at 0.38 by weight. The MS-to-FA replacement ratio used in this study is 1:5 or 20%. Sand is used as fine aggregates (1:1 precursor-aggregate ratio) and 20 mm length short bamboo fibers (1.4% fiber loading by weight) are used as reinforcement for the mortar coating in the fiber textile strengthening method.

The specimen variations and method of strengthening for each wallette sample are discussed in detail on the following sections.

2.3. Experimental Procedure

2.3.1. Preparation of Substrate

The substrate is the unreinforced masonry (URM) assembly made of clay bricks and cement-based in-fill mortars. The material specifications of the clay bricks and the in-fill mortars used are shown in Table 1. The clay bricks, 50 mm × 170 mm × 25 mm thick, are laid staggered inside 350 mm × 350 mm × 50 mm formworks made from phenolic boards to form the running bond layer of the masonry wallette. Sand with 3.5% moisture content is mixed with ordinary Portland cement (OPC), 1:6 cement-sand ratio by weight. For this mix, 0.4 water-cement ratio is used to obtain the workability of the in-fill mortar used in construction. The in-fill mortar is poured into the formworks with the laid bricks to form the URM substrate. Following these instructions, a total of 25 URM wallette substrates were prepared.

Table 1. In-fill mortar and clay bricks.

Material	Specification	Compressive Strength MPa (CoV [1])
In-fill mortar	1:6 cement–sand ratio	3.51 (11.44%)
Clay bricks	Moisture Content: 0.14%	4.52 (8.18%)

[1] CoV—Coefficient of Variance in %.

2.3.2. Preparation of Bamboo Fiber Textile

The bamboo fibers were prepared using the procedures discussed by Libre et al. [22]. Bamboo poles of *Bambusa blumeana*, or Kawayan Tinik, were cleaned with running water to remove excess dirt and starch. The poles were chopped into smaller slats to maximize the surface area that would be in contact with the sodium hydroxide (NaOH) solution that would be used to delignify the bamboo. Removing lignin that holds the fibers together makes it easier to disturb the bamboo and extract the fibers. The bamboo slats were submerged in 5% NaOH solution. After 24 h, a mechanical softening using rollers was used to extract the bamboo fibers. The extracted bamboo fibers were rinsed with water and treated with additional surface enhancing treatment, 10% aluminum sulfate ($Al_2(SO_4)_3$) solution for 36 h, to enhance the bonding between the fibers and the geopolymer matrix. Treated bamboo fibers were rinsed with water and air dried for at least 24 h. Portion of the treated bamboo fibers were cut into 20 mm lengths to produce the short bamboo fibers that will be the reinforcement for the geopolymer mortar coating. The remaining portion were prepared for textile-making. A total of 15 pieces of bamboo fiber textile grid were produced with 350 mm × 350 mm and 20 mm spacing of 2-ply 2–3 mm nominal diameter bamboo fiber cordages on both directions. The tensile capacity and tenacity, which is the measure of strength for natural fibers and is equal to the peak load that the fibers can resist in centiNewton (cN) over the fibers' fineness in Tex or in denier, were reported, as shown in Table 2.

Table 2. Tenacity of treated bamboo fibers (Kawayan Tinik).

Material	Specification	Tensile Strength (CoV [1])	Strain mm/mm (CoV)
Single strand	25 mmL bamboo fibers	16.624 cN/Tex (23%)	0.00271 (39%)
Single cordage	300 mmL, 2-ply 2–3 mm nominal diameter	27.61 cN/Tex (28%)	0.039 (18%)
Textile	20 mm spacing, 11 twines of single cord	11.7 kN/m	0.127

[1] CoV—Coefficient of Variance in %.

2.3.3. Preparation of Geopolymer Mortar for Coating

The geopolymer mortar that will be used as coating follows the mix proportion of the geopolymer paste discussed by Libre et al. [21] with the addition of sand and the short bamboo fibers as reinforcement. The average compressive strength of this geopolymer mortar mix is 3.08 MPa (CoV = 5%) with a split tensile strength of 0.74 MPa (CoV = 5.4%). To start, the mass precursors of 1:5 MS-to-FA ratio was prepared and estimated in order to fill 5 of the prepared wallette substrates for each run. This was to provide five samples of each with a uniform in-fill mix. This as repeated 5 times to fill all of the 25 prepared URM wallette substrates. In this study, 3200 g of FA, 800 g of MS, and 4000 g of sand was combined with a 1.4% bamboo fiber loading of 20 mm fiber length. Intervals of mixing for the addition of short fibers was carried out to minimize the clumping of fibers. The mass of NaOH and waterglass (1:2.5 NaOH-to-WG ratio) for the activator solution was determined using a 0.38 activator-to-precursor ratio. The water-solid ratio of 0.3 by mass was used to determine the amount of water to be used. Dissolved and cooled down NaOH flakes were mixed with waterglass and stirred for 5 min before setting aside. The solution was poured and mixed with the dry mix for 8 min using an automatic mortar mixer. The resulting bamboo fiber-reinforced geopolymer mortar mix was used as the coating for the strengthening method of the URM wallettes.

2.3.4. Strengthening Procedures and Specimen Nomenclature

The 25 URM wallete substrates were divided to 5 groups depending on the strengthening method to be used. Five wallettes remained unreinforced and used as control (C) samples. Five wallettes were plastered on one side with 20-mm-thick geopolymer mortar without bamboo fiber textile (S1). Five wallettes were plastered on both sides with 20-mm-thick geopolymer mortar without bamboo fiber textile (S2). Five wallettes were plastered on one side only with 10-mm-thick mortar before applying the bamboo fiber textile and coating it again with 10-mm-thick geopolymer mortar (BF1). The last five wallettes were plastered on both sides with 10-mm-thick mortar before applying the bamboo fiber textile and coating it again with 10-mm-thick geopolymer mortar to finish (BF2). Cling wrap was used as the curing technique following the curing technique used by Libre et al. [3]. The wrapped wallettes were left in an undisturbed area for ambient curing with temperature ranges from 34–38 °C, and relative humidity of 40 ± 5%, for 28 days before testing.

2.4. Diagonal Shear Test

After 28 days of curing, the wallettes were subjected to diagonal shear tests with orientation as shown in Figure 2. The test was administered using Shimadzu Universal Testing Machine (UTM) model AG-100kNXplus, displacement controlled at 5 mm/min rate. The load force and displacement parallel and perpendicular to the load were recorded using load cell (5 tons capacity) and Linear Variable Differential Transformer (LVDT) transducers, respectively. Both were connected to Almemo 710 Data Logger by Ahlborn.
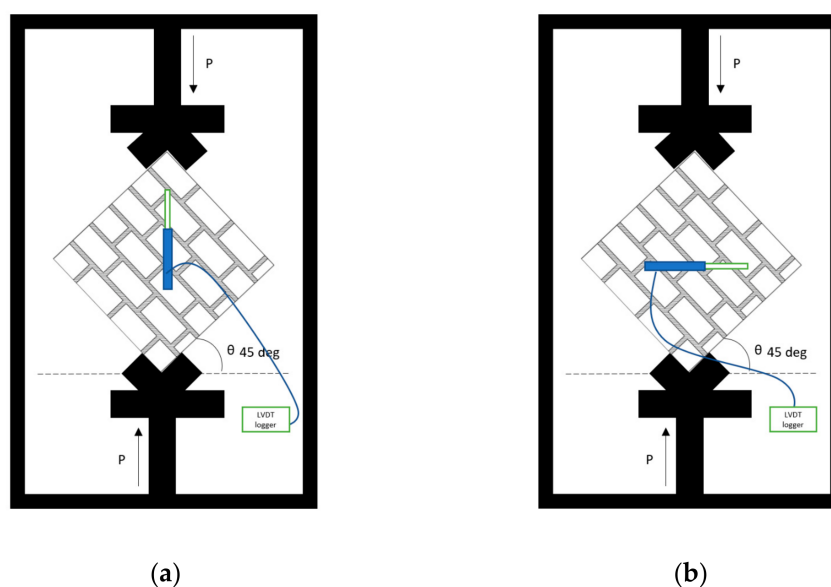

(**a**)   (**b**)

Figure 2. Diagonal shear test set-up: (**a**) front side LVDT set-up; (**b**) rear side LVDT set-up.

3. Results and Discussions

The results obtained from the tests described in the previous section are described in detail in the subsequent sections.

3.1. Experimental Results

The testing of wallette specimens was divided into groups with respect to the days that the coating of the strengthening was completed. The wallette specimens C, with no strengthening, served as the control samples and yielded the lowest peak load. For specimens C, the failure mode was running bond failure, where the crack propagated along the in-fill mortar running from the top of the diagonal and tracing the clay bricks, as shown in Figure 3b. This denotes the difference in compressive strength between the in-fill mortar and the clay bricks; the crack propagates and seeks the least resistance possible.
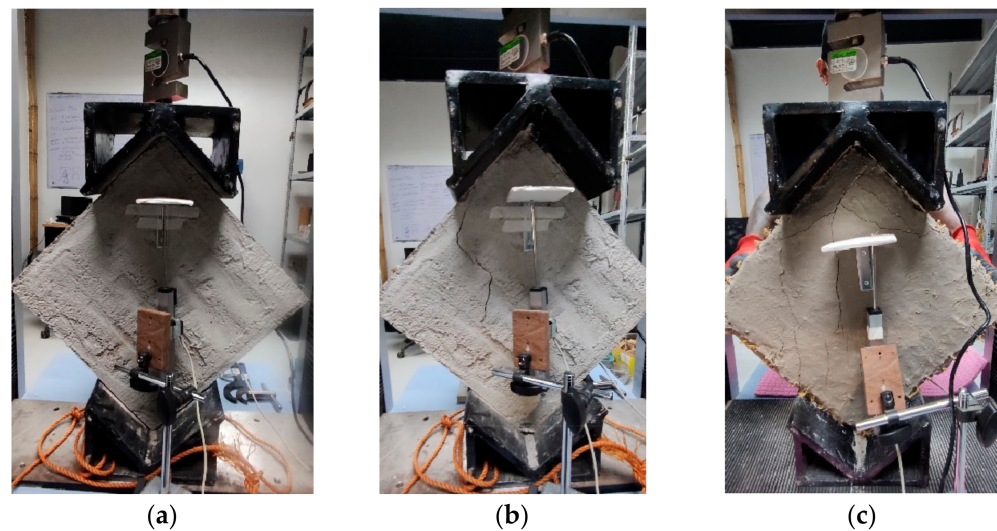
(a)   (b)   (c)

Figure 3. (**a**) Actual test set-up; (**b**) Failure mode of control sample; (**c**) Failure mode of BF1.

The failure mode seen on strengthened specimens S1 and BF1 follows a columnar crack pattern. As the forces acting on the specimens are being distributed, this results in forces acting perpendicular to the direction of initial load. This corresponds to internal tensile forces acting at the face of the specimen and generates the crack parallel to the direction of initial load, as shown in Figure 3c.

The summary of the experiment data gathered and computed results for the shear stress and shear strain using the Equations (2) and (3) is shown at Table 3. The results show a 12.04% and 24.92% increase in resisted shear force for specimens S1 and BF1, respectively. For specimens strengthened on both sides, S2 and BF2, the increase in the average shear force resisted was 17.57% and 35.80%, respectively.

Table 3. Experiment data and results.

Wallette Sample	Wallette Strengthening	Final Load (kN)	Ave. Shear Force kN (CoV [1])	Ave. Shear Stress MPa	Vert. Disp. mm	Hor. Disp. mm	Shear Strain mm/mm
C	Control	24.28	17.16 (24.68)	0.98	4.58	1.61	0.0125
S1	One-side	27.61	19.52 (7.83)	0.79	4.59	2.32	0.0139
BF1	One-side with textile	32.34	22.86 (27.57)	0.93	11.59	1.83	0.0271
S2	Two-side	29.46	20.82 (37.78)	0.66	7.87	2.76	0.0214
BF2	Two-side with textile	37.83	26.74 (5.72)	0.84	10.05	3.08	0.0265

[1] Coefficient of Variance in %.

3.2. Analysis of the Gathered Data

The deformation capacity of each of the specimens was calculated in terms of pseudo-ductility (μ) defined as the ratio of the ultimate shear strain and the calculated shear strain at cracking [15]. Oskouei et al. [16] defined the load and deformation at cracks as the points when the first appearance of cracks occurs. In the study of Sagar et al. [15], there were no defined points in the shear stress–strain diagram that could be used for shear stress and strain at cracking, thus, they took the shear stress at cracking as 0.75 times the peak stress and the corresponding strain as the shear strain at cracking [23,24]. In the current study, as there are no well-defined points to consider as the shear stress and strain at cracking, so the estimation of Sagar et al. [15] was considered. The modulus of rigidity, G_s, was computed as the ratio of shear stress and shear strain at cracking [15]. The summary of the modulus and pseudo-ductility of each wallette specimens are shown in Table 4.

Table 4. Shear stress, strain, modulus of rigidity, and pseudo-ductility.

Wallette Sample	Shear Stress at Cracking MPa	Shear Strain at Cracking mm/mm	G_s MPa	Pseudo-Ductility (μ)
C	0.688	0.0115	59.57	1.04
S1	0.658	0.0085	77.08	1.14
BF1	0.632	0.0241	26.15	1.21
S2	0.760	0.0181	41.87	1.36
BF2	0.678	0.0163	41.48	1.55

The increase in pseudo-ductility signifies the deformability of the material [15]. Based on the results as shown in Tables 3 and 4, the increase in load that the specimen can resist can be observed more evidently using the final peak load than the shear strength, as the value of shear stress is also dependent on the resulting total thickness of the wallette specimen; thus, there is almost no change in the computed shear strength. However, it is notable that the deformability of strengthened wallette specimens increased compared to the control sample. This signifies that the strengthening method used enhanced the ductility, which is more critical when considering strengthening or retrofitting schemes for masonry assemblages [15].

Oskouei et al. [16] presented the effect and behavior of their strengthening methods using load-displacement diagrams, while Shermi and Dubey [17] and Sagar et al. [15] presented the behavior through stress–strain diagrams. The load force (kN) versus vertical displacement (mm), as shown in Figure 4, shows the behavior of the specimen in the direction parallel to the direction of the load acting as shear force. The diagram shows an improvement of vertical displacement by 74.78% compared to the control samples C.
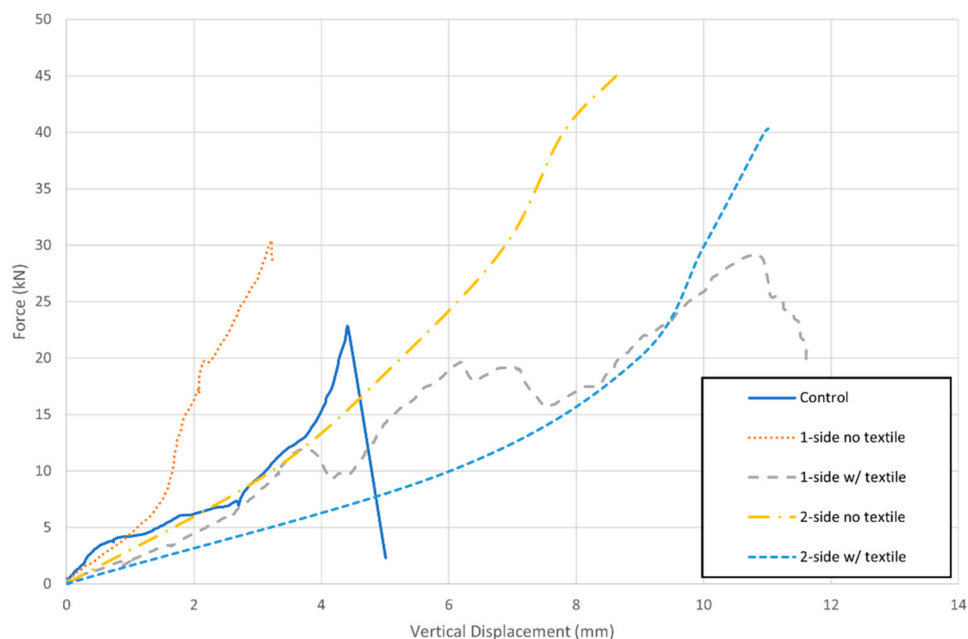
Figure 4. Load vs. displacement diagram of diagonal shear test.

The stress versus strain diagram, as shown in Figure 5, shows a more holistic approach, as the stress considered the shape of the specimen and the strain considered both vertical and horizontal displacements. It can be observed that the control samples C suffered brittle failure after reaching peak load. This is supported with the pseudo-ductility value computed for the control samples, which is 1.04, as shown in Table 4. This signifies that there is almost no difference between the peak strain and the strain at cracking, thus confirming that the specimens failed right after the peak load. The strengthened specimens sustained larger deformation compared to the control samples, even after the estimated strain at cracking.
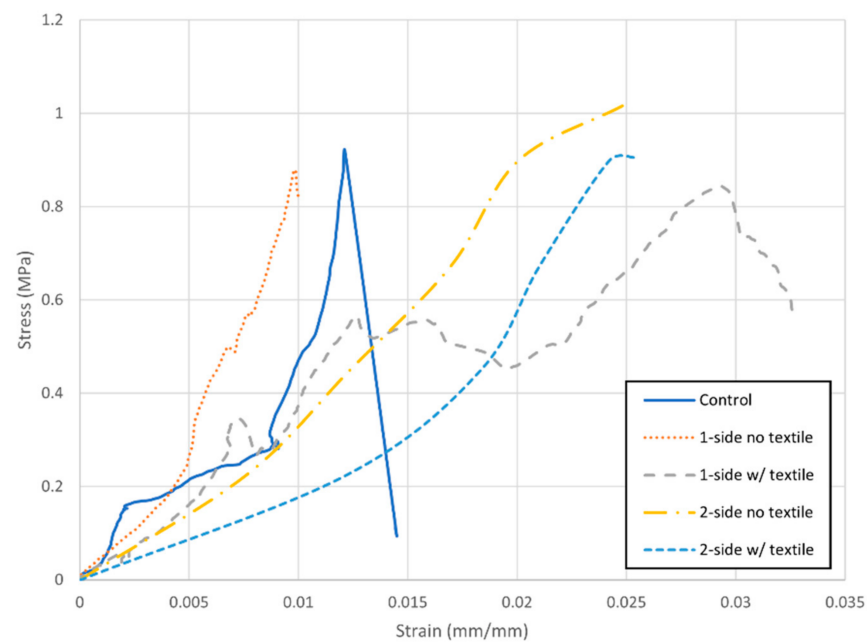
Figure 5. Stress vs. strain curve of diagonal shear test.

3.3. Other Factors

The results of the diagonal shear tests are influenced by external factors from the data gathering up until the analysis of data. This sub-section includes qualitative assessment and recommendations for future studies that can help researchers who might consider using small wallette specimens as their method of investigating the in-plane behavior of assembly walls.

There are factors that might have influenced the occurrence of deviations and variance in results (5.72% to 37.78% CoV for shear forces recorded). Minor factor such as workmanship for the installation of the strengthening method can be minimized through practice, mastering the application of mortar as coating to walls. The bond of the geopolymer mortar used as coating to the clay brick wall substrate is also important to look at. As shown in Figure 6a, some of the tested specimens of BF1 suffered debonding of the mortar, leaving the substrate to fail while the textile reinforcement was still intact. This might happen when poor adhesion is present and can be minimized by proper surface preparation before the application of mortar coating. Testing of bond strength can be carried out separately to further evaluate the mortar bond to substrate [15].
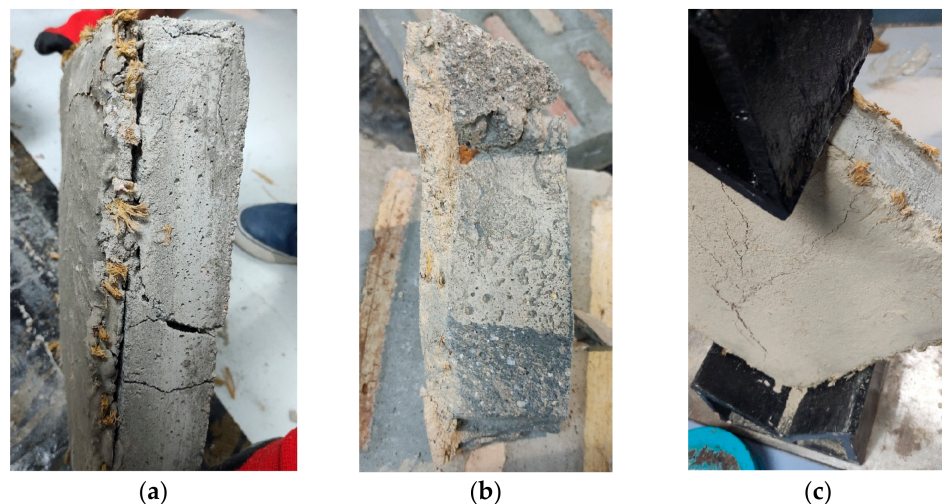

Figure 6. (**a**) Failure on bond BF1; (**b**) Bond still intact S1; (**c**) Failure mode of BF2.

4. Comparison between Analytical and Experimental Results

In terms of applying the data from the discussed experiments for retrofitting masonry walls, there are some additional tests to consider. The American Concrete Institute (ACI) introduced ACI 549.4R, a guide to the design and construction of externally bonded fabric-reinforced cementitious matrix for masonry structures [25]. As it is more established, some authors [7,15,24] made use of the existing analytical models from ACI 549.4R to estimate the in-plane shear strength of strengthened masonry walls. The general idea is governed by the equation,

$$Vn = Vm + (Vfm \; or \; Vft) \tag{4}$$

where Vn is the nominal shear capacity, Vm is the contribution of the masonry wall, and Vft and Vfm are the shear capacities of the strengthening method with and without textile, respectively.

The shear contribution of the masonry, Vm, is calculated using the equation,

$$Vm = (fvd)(d)(t) \tag{5}$$

where fvd is the average shear stress based on control samples C, d is length of one side of the wallette, and t is the thickness of the wallette.

The shear contribution of the strengthening method with short bamboo fiber-reinforced geopolymer mortar but without the geotextile, Vfm, is calculated by the equation,

$$Vfm = (s)(fvs)(d)(t), \tag{6}$$

where s is the number of sides strengthened, fvs is the average shear stresses of wallettes (S1 and S2), d is the length of one side, and t is the thickness of the wallette.

The shear contribution of the strengthening method with geotextile coated with the short bamboo fiber-reinforced geopolymer mortar, Vft, is defined and calculated using ACI 549.4R approach and is governed by the equation,

$$Vft = (s)(n)(A_f)(L)(E_f)(\varepsilon fv), \tag{7}$$

where s is the number of sides strengthened, n is the number of strengthening mortar layer, A_f is the area of the externally bonded strengthening mortar, L is the length of the wall, E_f is the modulus of elasticity of cracked strengthened mortar, and ε_{fv} is the value of ultimate tensile strain of the strengthened mortar—but not more than 0.004. ε_{fv} is the strain considered from a separate tensile test on coupons for the reinforced mortars with textiles [15]. However, if we are to consider the ultimate tensile strain that can be resisted by the textile used in the current study as shown in Table 2, which is 0.127 mm/mm, we can consider ε_{fv} as 0.004.

The nominal shear Vn is analytically computed and compared with the shear in experimental results, $Vexp$, discussed in previous sections. The summary of the contributions and the experimental/analytical ratio ($Vexp/Vn$) is shown in Table 5.

Table 5. Comparison between analytical and experimental results.

Wallette Sample	*Vexp* (kN)	*Vm*	*Vfm*	*Vft*	*Vn*	*Vexp/Vn*
C	17.16	17.15	-	-	17.15	1.001
S1	19.52	17.15	5.53	-	22.68	0.861
BF1	22.86	17.15	-	2.24	19.39	1.179
S2	20.82	17.15	9.24	-	26.39	0.789
BF2	26.74	17.15	-	7.11	24.26	1.102

The accuracy of the model in predicting the added shear capacity using the strengthening method is denoted by the nearness of *Vexp/Vn* to 1. Comparing with the *Vexp/Vn*

ratio of 1.48 by Sagar et al. [15], who used the same ACI 549.4R approach, the results of the models in the current study are more accurate in calculating the nominal shear capacity and contributions of each strengthened URM. As there are no standards to follow when using bamboo fiber geotextile and short bamboo fiber-reinforced geopolymer mortar, the equations presented deemed usable for design purposes.

5. Conclusions and Recommendations

In this study, the performance of a bamboo fiber textile-reinforced geopolymer mortar system in strengthening the in-plane shear strength of URM wall assemblages is investigated through diagonal shear tests. Fibers extracted from Kawayan Tinik and treated with 10% aluminum sulfate were used to produce cordages and textiles to reinforce URM wallette specimens, 350 mm $\times$ 350 mm, made of clay bricks and in-fill mortar. Mill scale and fly ash based geopolymer reinforced with short bamboo fibers were used as mortar coating for the textile reinforcement.

It was observed that strengthening both sides with bamboo textile coated with bamboo fiber-reinforced MS-FA geopolymer mortar increased the average shear force that the walls could resist by 35.80% or 9.58 kN more than the 17.16 kN of URM control samples. An improvement of vertical displacement of 74.78% was also observed for BF2 compared to the control samples C.

There was an increase in deformability of the walls that was expressed by the pseudo-ductility value for S2 and BF2 specimens. From 1.04 of control samples, the pseudo-ductility of BF2 increased up to 1.55, which suggests that the samples still experienced further deformation even after the initial cracking. This signifies that the strengthening method used enhanced the ductility and is important when considering strengthening or retrofitting masonry assemblages.

To maximize the impact of the proposed strengthening method, it is recommended for future studies to conduct cost-benefit analysis, comparing different existing strengthening methods. It is also recommended that the bond between the proposed geopolymer mortar and the substrate be included as part of the optimization in material development.

The results presented on this paper can be used as basis of modulus of rigidity, G_s, and maximum tensile strength of bamboo fiber textiles for strengthening masonry walls, given that the bamboo fibers and the geopolymer mortar to be used are the same.

Author Contributions: Conceptualization, R.G.D.L.J. and J.M.C.O.; methodology, R.G.D.L.J. and J.M.C.O.; validation, J.L.L.J., J.M.C.O. and L.F.L.; formal analysis, R.G.D.L.J. and J.M.C.O.; investigation, R.G.D.L.J., C.J.D.C., J.L.L.J. and J.M.C.O.; resources, L.F.L., and R.G.D.L.J.; data curation, R.G.D.L.J.; writing—original draft preparation, R.G.D.L.J.; writing—review and editing, R.G.D.L.J., J.L.L.J., L.F.L., C.J.D.C., M.A.B.P., E.J.G., L.E.O.G. and J.M.C.O. All authors have read and agreed to the published version of the manuscript.

Data Availability Statement: The data presented in this study are available on request from the corresponding author.

Conflicts of Interest: The authors declare no conflict of interest.

References

1. Lucchini, S.S.; Facconi, L.; Minelli, F.; Plizzari, G. Retrofitting unreinforced masonry by steel fiber reinforced mortar coating: Uniaxial and diagonal compression tests. *Mater. Struct.* **2020**, *53*, 144. [CrossRef]
2. Parisi, F.; Augenti, N. Earthquake damages to cultural heritage constructions and simplified assessment of artworks. *Eng. Fail. Anal.* **2013**, *34*, 735–760. [CrossRef]

3.   D'Ayala, D.; Speranza, E. Definition of collapse mechanisms and seismic vulnerability of historic masonry buildings. *Earthq. Spectra* **2003**, *19*, 479–509. [CrossRef]

4.   Dhanasekar, M. Shear in reinforced and unreinforced masonry: Response, design and construction. *Procedia Eng.* **2011**, *14*, 2069–2076. [CrossRef]

5.   Ghezelbash, A.; Beyer, K.; Dolatshahi, K.M.; Yekrangnia, M. Shake table test of a masonry building retrofitted with shotcrete. *Eng. Struct.* **2020**, *219*, 110912. [CrossRef]

6.   Messali, F.; Metelli, G.; Plizzari, G. Experimental results on the retrofitting of hollow brick masonry walls with reinforced high performance mortar coatings. *Constr. Build. Mater.* **2017**, *141*, 619–630. [CrossRef]

7.   Babaeidarabad, S.; Arboleda, D.; Loreto, G.; Nanni, A. Shear strengthening of un-reinforced concrete masonry walls with fabric-reinforced-cementitious-matrix. *Constr. Build. Mater.* **2014**, *65*, 243–253. [CrossRef]

8.   Carozzi, F.G.; Poggi, C. Mechanical properties and DEBONDING strength of FABRIC Reinforced Cementitious MATRIX (FRCM) systems for MASONRY strengthening. *Compos. Part B Eng.* **2015**, *70*, 215–230. [CrossRef]

9.   Corradi, M.; Borri, A.; Castori, G.; Sisti, R. Shear strengthening of wall panels through jacketing with cement MORTAR reinforced by GFRP GRIDS. *Compos. Part B Eng.* **2014**, *64*, 33–42. [CrossRef]

10. Lourenço, P. Recommendations for restoration of ancient buildings and the survival of a masonry chimney. *Constr. Build. Mater.* **2006**, *20*, 239–251. [CrossRef]

11. ICOMOS, Recommendations for the Analysis, Conservation and Structural Restoration of Architectural Heritage, 2001. Available online: https://ancientgeorgia.files.wordpress.com/2012/04/recommendations_icomos-principles-and-guidelines.pdf (accessed on 1 December 2022).

12. Petrozzi, G.R.; Carbajal, F.; Schexnayder, C.J. Restoration of a historic adobe church. *Pract. Period. Struct. Des. Constr.* **2015**, *20*, 04014026. [CrossRef]

13. Blondet, M.; Vargas, J.; Tarque, N. Observed behaviour of earthen structures during the Pisco (Perú) earthquake of August 15, 2007. In Proceedings of the 14th World Conf. Earthquake Engineering, Beijing, Earthquake Engineering Research Institute (EERI), Oakland, CA, USA, 12–17 October 2008; Available online: http://www.eeri.org/lfe/pdf/peru_pisco_adobe.pdf (accessed on 1 December 2022).

14. *ASTM E519-02*; Standard Test Method for Diagonal Tension (Shear) in Masonry Assemblages. ASTM International: West Conshohocken, PA, USA, 2002. Available online: www.astm.org (accessed on 1 February 2021).

15. Sagar, S.L.; Singhal, V.; Rai, D.C.; Gudur, P. Diagonal shear AND OUT-OF-PLANE flexural strength of fabric-reinforced Cementitious Matrix–Strengthened Masonry Wallettes. *J. Compos. Constr.* **2017**, *21*, 04017016. [CrossRef]

16. Oskouei, A.V.; Jafari, A.; Bazli, M.; Ghahri, R. Effect of different retrofitting techniques on in-plane behavior of masonry wallettes. *Constr. Build. Mater.* **2018**, *169*, 578–590. [CrossRef]

17. Shermi, C.; Dubey, R. In-plane behaviour of unreinforced masonry panel strengthened with welded wire mesh and mortar. *Constr. Build. Mater.* **2018**, *178*, 195–203. [CrossRef]

18. *ASTM C67/C67M-20*; Standard Test Methods for Sampling and Testing Brick and Structural Clay Tile. ASTM International: West Conshohocken, PA, USA, 2020. Available online: www.astm.org (accessed on 1 February 2021).

19. *ASTM C780-20*; Standard Test Method for Preconstruction and Construction Evaluation of Mortars for plain and Reinforced Unit Masonry. ASTM International: West Conshohocken, PA, USA, 2020. Available online: www.astm.org (accessed on 1 February 2021).

20. *ASTM C270-19ae1*; Standard Specification for Mortar for Unit Masonry. ASTM International: West Conshohocken, PA, USA, 2019. Available online: www.astm.org (accessed on 1 February 2021).

21. Libre, R.G.D., Jr.; Garciano, L.E.O.; Promentilla, M.A.B.; Guades, E.J.; Ongpeng, J.M.C. Compressive Strength and Setting Time of Mill Scale-Low Calcium Fly Ash Based Geopolymer Paste. *Chem. Eng. Trans.* **2022**, *94*, 175–180. [CrossRef]

22. Libre, R.G., Jr.; Promentilla, M.A.; Garciano, L.; Lejano, B.; Winston Oreta, A.; Ongpeng, J.M.; Guades, E.; Leaño Jr., J.; Cruz, A.Z.; Lopez, L.F. Mechanical performance of treated Bambusa Blumeana (bamboo) fibers. In Proceedings of the IABSE Symposium, Prague 2022: Challenges for Existing and Oncoming Structures, Prague, Czech Republic, 25–27 May 2022. [CrossRef]

23. Papanicolaou, C.G.; Triantafillou, T.C.; Karlos, K. Textile-reinforced mortar (TRM) versus FRP as strengthening material of URM walls: In-plane cyclic loading. *Mater Struct* **2007**, *40*, 1081–1097. [CrossRef]

24. Babaeidarabad, S.; De Caso, F.; Nanni, A. URM walls strengthened with fabric-reinforced cementitious matrix composite subjected to diagonal compression. *J. Compos. Constr.* **2014**, *18*, 04013045. [CrossRef]

25. *ACI 549.4R-13*; Guide to Design and Construction of Externally Bonded Fabric-Reinforced Cementitious Matrix (FRCM) Systems for Repair and Strengthening Concrete and Masonry Structures. American Concrete Institute: Farmington Hills, MI, USA, 2013. Available online: https://www.concrete.org/ (accessed on 1 December 2022).